# Comparative effects of biologically synthesized Zn and Cu NPs on callus induction and physiological traits of chicory (Cichorium intybus) in vitro

**Mohammad Reza Asgharipour**

moasgharipour@gmail.com

University of Zabol https://orcid.org/0000-0001-7197-6578

**Hamideh Khajeh**

University of Zabol

**Bahman Fazeli-Nasab**

University of Zabol

**Ali Salehi Sardoei**

AREEO: Agricultural Research Education and Extension Organization

**Zeinab Fotoohiyan**

: Islamic Azad University Kerman Branch

**Ali Reza Mirzaei**

University of Mohaghegh Ardabili

**Research Article**

**Keywords:** Green synthesis of metal, Moringa plant, Chicory, Pathway analysis, Tissue culture

**Posted Date:** November 18th, 2025

**DOI:** https://doi.org/10.21203/rs.3.rs-8012165/v1

# Comparative effects of biologically synthesized Zn and Cu NPs on callus induction and physiological traits of chicory (*Cichorium intybus*) *in vitro*

**Hamideh Khajeh[1], Bahman Fazeli-Nasab[2], Ali Salehi Sardoei[3,*], Zeinab Fotoohiyan[4], Ali Reza Mirzaei[5], Mohammad Reza Asgharipour[6*]**

[1]Agriculture Biotechnology Research Institute, University of Zabol, Zabol, Iran; hmdekhaje@yahoo.com
[2]Department of Agronomy and Plant Breeding, Agriculture Institute, Research Institute of Zabol, Zabol, Iran; bfazelinasab@gmail.com
[3]Department of Horticultural and Crops Research, Southern Kerman Agricultural and Natural Resources Research and Education Center, AREEO, Jiroft, Iran.
[4]Department of Plant Pathology, Jiroft Branch, Islamic Azad University, Kerman, Iran.
[5]Department of Agronomy and Plant Breeding, Faculty of Agriculture and Natural Resources, University of Mohaghegh Ardabili, Ardabil, Iran; amirzaei25@gmail.com
[6]Department of Agronomy, College of Agriculture, University of Zabol, Zabol, Iran; m_asgharipour@uoz.ac.ir

* Corresponding authors: alisalehisardoei@gau.ac.ir (A. Salehi Sardoei), M.R. Asgharipour (m_asgharipour@uoz.ac.ir)

## Abstract

This study investigated the properties of copper (Cu) and zinc (Zn) nanoparticles (NPs) biosynthesized using the aqueous extract of moringa. The size and structure of the metal NPs derived from the moringa plant aqueous extract were confirmed using transmission electron microscopy (TEM), scanning electron microscopy (SEM), X-ray diffraction (XRD), and Fourier transform infrared spectroscopy (FT-IR). Chlorophyll a, b, total chlorophyll, carotenoids, proline, and fresh and dry weights of callus were measured. The study aimed to optimize callus production in chicory by first synthesizing Zn and CuNPs using moringa aqueous extract. The size and structure of the biosynthesized Zn and CuNPs were then examined using SEM and XRD. Subsequently, the effects of different concentrations of these biosynthesized Zn and CuNPs on chlorophyll a, b, total chlorophyll, carotenoids, proline, and fresh and dry weights of callus were evaluated under *in vitro* culture conditions. Electron microscopy images confirmed the synthesis of Cu and ZnNPs, which were spherical with average particle sizes of 8 nm and 12 nm, respectively. The highest values for chlorophylls, fresh weight, and dry weight of callus were obtained with 100 mg/l CuNPs. The highest proline content was achieved with 150 mg/l CuNPs, while the highest carotenoid content was observed with 100 mg/l ZnNPs. Overall, the use of Cu and ZnNPs demonstrated that the strongest positive direct effects were on proline (0.708) and callus fresh weight (1.091), whereas the weakest direct effects, which were negative, were on chlorophyll b (−0.218) and chlorophyll a (−0.605).

**Keywords**: Green synthesis of metal; Moringa plant; Chicory; Pathway analysis; Tissue culture

## Key Message

Green-synthesized Cu and Zn nanoparticles from moringa extract enhance chicory callus growth, pigments, and proline at optimal 100–150 mg/L doses.

## Introduction

Chicory, a medicinal plant with the scientific name *Cichorium intybus* L., belongs to the Asteraceae family and is native to the Mediterranean region. This plant has been used as a home remedy for various diseases since ancient times (Singh and Chahal 2018). It is also utilized in indigenous medicine to treat various ailments and possesses multiple medicinal properties, including antioxidant, antimicrobial, anti-diabetic, anti-inflammatory, prebiotic, cardioprotective, and immune-boosting effects (Das et al. 2016). Chicory contains compounds such as alkaloids, inulin, lactones, sesquiterpenes, coumarins, flavonoids, chicoric acid, and vitamins (Street et al. 2013).

NPs are primary particles smaller than 100 nm. Today, nanotechnology stands as one of the most advanced technologies, permeating all facets of human, animal, plant, environmental, and industrial life. The rise of nano-innovation has significantly impacted both current and future scenarios, akin to the transformative effects of the steam engine and the Internet. It has fostered the talent and potential to drive fundamental changes across various scientific and industrial sectors (Azim et al. 2023). The result of human activities is the introduction of nanoparticles (NPs) into the environment. There is still no accurate information about the impact of these substances on the environment and their toxic effects (Largia et al. 2022).

Studies on the toxicity of NPs in plants indicate disruption in seed germination and plant growth. Available studies show different reactions of plant species to nano-formulated nutrients. For example, it has been shown that *Linum usitatissimum* growing in an aqueous environment containing NPs can absorb, translocate, and accumulate particles in plant tissues (Karimzadeh et al. 2019). On the other hand, cucumber is unable to absorb and transport NPs (Ghani et al. 2022). Therefore, different plants exhibit varied responses to NPs (Khajeh et al. 2023; Alavi and Hamblin 2023; Alavi et al. 2022a, b). There are limited reports on the positive effects of nano-fertilizers on the growth of some plants, including lettuce and sweet pepper (Kalisz et al. 2021), *Stevia rebaudiana* (Javed et al. 2018), wheat (Feng et al. 2022), tomato (Ahmed et al. 2023) and amaranth (Cai et al. 2022). Copper (Cu) is a low-use but essential element for all higher plants, similar to iron in terms of oxidation-reduction properties and the formation of highly stable complexes (Ghorbanpour et al. 2021). Divalent copper can be rapidly reduced to monovalent copper. The important role of copper as a nutrient is due to its participation in the structure of key enzymes and in electron transfer during oxidation-reduction reactions. Due to its high affinity for forming bonds with different groups, more than 98–99% of copper exists as complexes in plants (Huang et al. 2019).

Copper toxicity in plants is significant from two perspectives: first, crops are generally highly sensitive to Cu toxicity; second, Cu accumulation in agricultural soils is a common issue in modern agriculture due to the use of industrial herbicides and fungicides, as well as the discharge of industrial wastewater and sewage into fields (Baskar et al. 2018). Copper toxicity affects various physiological and biochemical processes in plants, most notably photosynthesis, pigment synthesis, protein metabolism, and membrane integrity. Exposure to copper induces stress, disrupting the plant's water balance. Additionally, copper toxicity can lead to proline accumulation in plant tissues, a well-documented phenomenon in numerous plant species (Ahmad et al. 2020).

Low concentrations of copper and zinc increase root and shoot growth in *Stevia rebaudiana* (Javed et al. 2018). During experiments, Zn NPs enhanced root growth compared to control seedlings (Iziy et al. 2019). Copper NPs (CuO) have recently been recognized as antimicrobial agents. The bactericidal properties of NPs depend on their size, stability, and concentration used as antibacterial agents (Chung et al. 2019). Highly ionic CuO and ZnO NPs can be synthesized in crystalline morphologies with high specific surface area (Javed et al. 2018; Abhilash et al. 2023).

The chicory plant (*C. intybus* L.) is an important medicinal plant with valuable secondary metabolites. Chicory callus serves as a good source for the production and extraction of these metabolites. In this research, changes in chicory callus were investigated in terms of morphological and biochemical characteristics to identify the optimal treatment.

## Materials and methods

### Preparation and disinfection

Chicory plant seeds were procured from Pakan Seed Company in Isfahan and washed under running water for 30 minutes to prepare sterile seedlings. Then, under a laminar hood, they were immersed in 70% ethanol for 90 seconds, followed by treatment with 5% sodium hypochlorite solution containing a few drops of Tween 80 for 25 minutes. Subsequently, the seeds were rinsed twice with sterile distilled water for 15 minutes each and placed on clean sterile paper until the surface water was completely dry (Koohsari et al. 2020). Finally, the sterilized seeds were inoculated onto MS basal medium containing 20 g/L sucrose for germination and incubated in a growth chamber under 16 hours of light and 8 hours of darkness at 25 ± 2 °C (Figure 1). After germination and seedling growth, they were used as a source of explants to obtain callus.

**Figure 1.** Preparation of rhizome to obtain callus in chicory plant

**Preparation of aqueous extract**

First, *Moringa* (*Moringa oleifera*) plant leaves were collected from Zabol city with the approval of the Sistan and Baluchestan Natural Resources Department. The voucher specimen (*M. oleifera*) was confirmed by Dr. Mehdi Dehghani from the Department of Biology, University of Zabol, Iran, and assigned the herbarium code UOZH1512. Then, after washing, the leaves were dried in the shade and milled. The extract was prepared by adding 20 g of moringa powder to 100 ml of deionized water in a beaker and heating in a water bath at 80 °C for 70 minutes to obtain the primary extract. The resulting blue extract was filtered using Whatman No. 1 paper and a syringe filter, then stored in Falcon tubes in dark bottles at 4°C (Nikbakht and Pour Ali 2015).

.

**Synthesis of zinc nanoparticles**

To synthesize Zn NPs using the green method, 5 g of zinc nitrate was added to 10 ml of the extract, and the solution was heated to yield a white powder containing Zn NPs. The accuracy of NP synthesis was evaluated using XRD and scanning electron microscopy (SEM) (Kumar et al. 2013).

**Synthesis of copper nanoparticles**

Seventy-five milliliters of freshly prepared extract was added to 100 ml of 0.01 M copper sulfate solution with constant stirring and maintained at 60 °C for 24 hours (Roy et al. 1999). The mixture was then centrifuged at 12,000 rpm for 20 minutes, and this process was repeated twice to remove impurities. The color change from green to amber-yellow indicated NP formation. The synthesized NPs were dried in an oven at 60 °C for further analysis (Tahvilian et al. 2019).

**Properties of synthesized nanoparticles**

Transmission electron microscopy (TEM) analysis was performed at 70 kV accelerating voltage to determine particle size and shape. A drop of the NPs solution was placed on a copper grid and dried at room temperature by water evaporation. The size and morphology of Cu and Zn NPs were examined using SEM. Crystalline properties, structure, and crystal size of CuO NPs were analyzed by XRD using a Rigaku-Miniflex X-ray diffractometer (Rigaku Corporation, Tokyo, Japan) with Cu-Kα radiation ($\lambda = 0.15406$ nm) over a $2\theta$ range of 20° to 80°. SEM analysis was conducted using The JEOL JSM5600 system (JEOL Ltd., Tokyo, Japan). For electron microscopy, the reaction mixture was centrifuged three times at 12,000 rpm for 15 minutes. A few drops of the resulting pellet were dried on aluminum foil at room temperature, and images were captured. To identify biomolecules responsible for NP reduction and capping, FT-IR analysis was performed at room temperature using a Nicolet 6700 FTIR spectrometer**.**

**Preparation of MS culture medium**

To investigate the effects of Cu and Zn NPs on chicory callus formation in October 2024, fresh green leaves from plants in the greenhouse of Zabol University's Faculty of Agriculture were used as explants. Explants were

disinfected with 5% sodium hypochlorite containing five drops of Tween 23 for seven minutes, then rinsed three times with deionized water for five minutes each (Mezginezhad et al. 2019). MS medium was prepared by dissolving 17.215 g of MS powder in 500 ml of deionized water, adjusting the volume to 1 L, and setting the pH to 8.5 using NaOH or 1 N HCl. One milliliter of 10% ascorbic acid was added. The medium was distributed into 250 ml flasks, supplemented with 1% BAP and 2IP, and 8 g/L agar. Flasks were capped with aluminum foil and autoclaved at 121 °C and 1.5 atm for 20 minutes under a laminar hood.

After sterilization, leaf explants were cut into uniform pieces and transferred to jars containing solidified medium. Jars were sealed with parafilm and incubated at 22°C in complete darkness for one month (Mezginezhad et al. 2019). Callus formation occurred after one month, and calluses were subcultured onto medium containing the treatments for two months.

**Callus induction in chicory plant**

After 30 ± 5 days, when plants had grown sufficiently, leaf samples were prepared and cut into 1 cm segments. To optimize callus induction, MS medium was supplemented with different concentrations of Cu NPs (0, 100, 150, and 200 mg/l) and Zn NPs (0, 100, 150, and 200 mg/l) in three replications. Samples were incubated at 25 ± 2 °C under 16 hours light/8 hours darkness.

**Traits measurement**

The experiment followed a completely randomized design with three replications. Measured traits included chlorophylls (a, b, total, and carotenoids), proline, and fresh and dry weights of callus. Chlorophyll and carotenoid contents were determined using the method of Barnes et al. (1992). Half a gram of fresh leaf sample from each treatment was incubated in 10 ml dimethylsulfoxide (DMSO) at 70 °C for three hours until pigments were fully extracted and tissue became colorless. Then, 250 µL of extract was diluted with 2 mL DMSO. Absorbance was measured using a spectrophotometer with pure DMSO as blank. Chlorophyll a, b, total chlorophyll, and carotenoids were calculated at 663, 645, 480, and 510 nm, respectively, using Eqs. (1-4):

$$\text{Chl a (mg/g. F.w)} = 12.7(A663) - 2.69(A645) \times V/1000 \times W \quad (1)$$

$$\text{Chl b (mg/g. F.w)} = 22.7(A645) - 4.68(A663) \times V/1000 \times W \quad (2)$$

$$\text{Chl total (mg/g. F.w)} = 20.2(A645) - 8.02(A663) \times V/1000 \times W \quad (3)$$

$$\text{Carotenoids (mg/g. F.w)} = 7.6(A480) - 1.49(A510) \times V/1000 \times W \quad (4)$$

where A = absorbance at the indicated wavelength, V = final volume of solution, and W = sample fresh weight.

For proline measurement, 0.1 g of dried sample was ground in a mortar with 10 ml of 3% sulfosalicylic acid. The extract was filtered and stored on ice. Two milliliters of ninhydrin reagent (1.25 g ninhydrin, 20 ml 6 M phosphoric acid, 30 ml glacial acetic acid) and 2 ml glacial acetic acid were added to 2 mL of extract. Tubes were heated at 100 °C for one hour in a water bath, then cooled on ice. Six milliliters of toluene was added, and tubes were shaken vigorously for 15–20 seconds. The upper phase was read at 520 nm using a spectrophotometer. Proline concentration was determined using a standard curve and expressed as µmol/g (Sena et al. 2024). Fresh and dry weights of callus were measured using a digital scale with 0.001 g precision.

**Statistical analysis**

The experiment was conducted in a completely randomized factorial design with three replications. Statistical analysis began with descriptive statistics to assess data quality. Data were summarized to simplify interpretation. Duncan's multiple range test (DMRT) was performed using SPSS software (version 26; IBM Corp., Armonk, NY, USA) at $p \leq 0.05$ to compare means and detect significant differences. Pearson's correlation coefficients were calculated to evaluate relationships between traits. Stepwise regression analysis was conducted at $p < 0.01$ to identify key traits influencing performance. Path analysis was used to determine direct and indirect effects of traits in the model, focusing on those explaining the most variation. All analyses (data normality, correlation, stepwise regression, and path analysis) were performed using SPSS version 26.

**Results**

**Photosynthesis and parameter optimization for the synthesis of Zinc Oxide and Copper nanoparticles**

Zinc oxide nanoparticles (ZnO NPs) were synthesized using green synthesis methods, with plant extracts serving as reducing and stabilizing agents. *Cichorium intybus* leaf extract was used to reduce zinc nitrate to ZnO NPs under optimized conditions (pH 9–11, 60–80°C). The formation of ZnO NPs was confirmed by UV-Vis spectroscopy, showing a characteristic absorption peak at 365–375 nm due to their bandgap energy (~3.3 eV). The green synthesis approach avoided toxic chemicals, making it environmentally friendly (Figure 2, left). Copper nanoparticles (Cu NPs) were synthesized via biological reduction using plant extracts such as *Ocimum sanctum* or fungi. The reduction of copper sulfate ($CuSO_4$) to $Cu^0$ was monitored by UV-Vis spectroscopy, revealing a surface plasmon resonance (SPR) peak at 555–570 nm. Optimal synthesis conditions included a temperature of 50–70°C, pH 7–9, and a 1:4 molar ratio of precursor to extract (Figure 2, right). The following factors influencing ZnO NPs

and Cu NPs synthesis were then investigated to produce NPs with more uniform morphology and smaller size: reaction time, extract volume, pH of the reaction solution, and concentration of precursor salt.

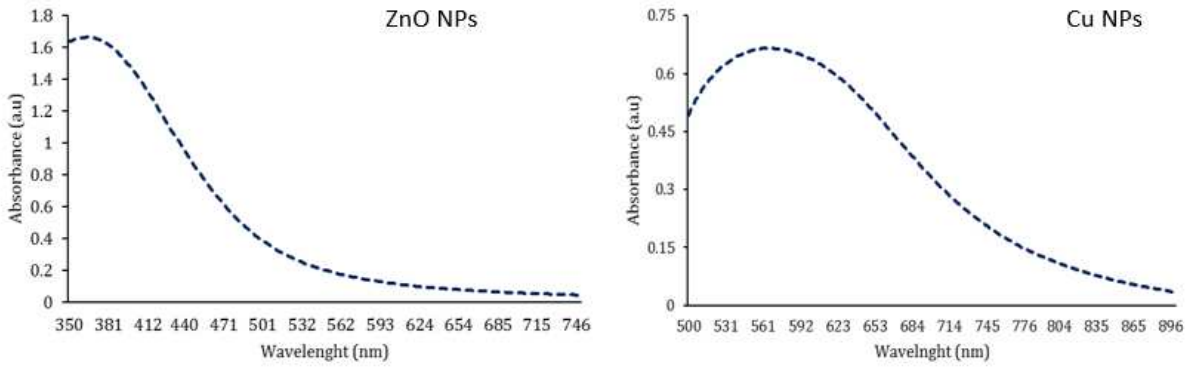


**Figure 2.** Visible-ultraviolet spectrophotometer spectrum of Zinc oxide nanoparticles (left) and Copper nanoparticles (right) synthesized with chicory (*Cichorium intybus*) plant extract**.**

**Properties of synthesized nanoparticles**

The size and morphology of synthesized Cu and Zn NPs were investigated using transmission electron microscopy (TEM) and scanning electron microscopy (SEM). Results showed that Cu and Zn NPs produced via green synthesis were highly homogeneous and spherical, with average particle sizes of 8 nm and 12 nm, respectively (Figures 3 and 4).

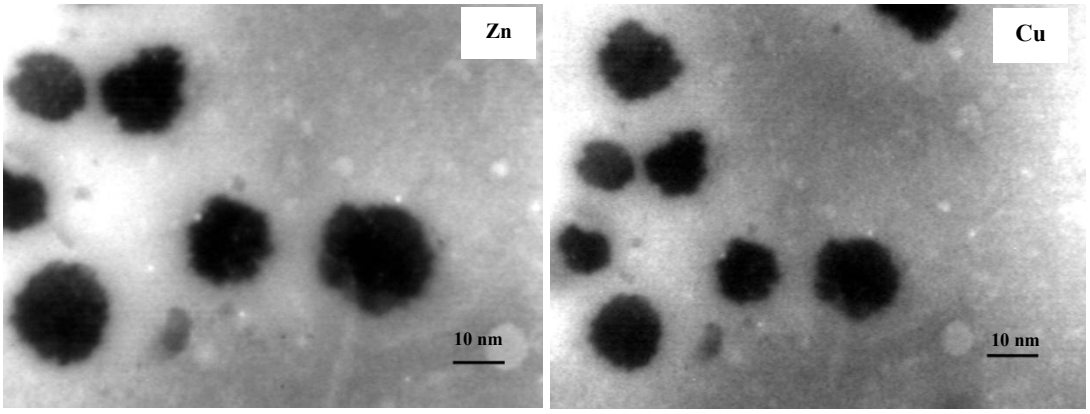


**Figure 3.** Transmission electron microscope image of Cu and Zn NPs synthesized by moringa plant aqueous extract.

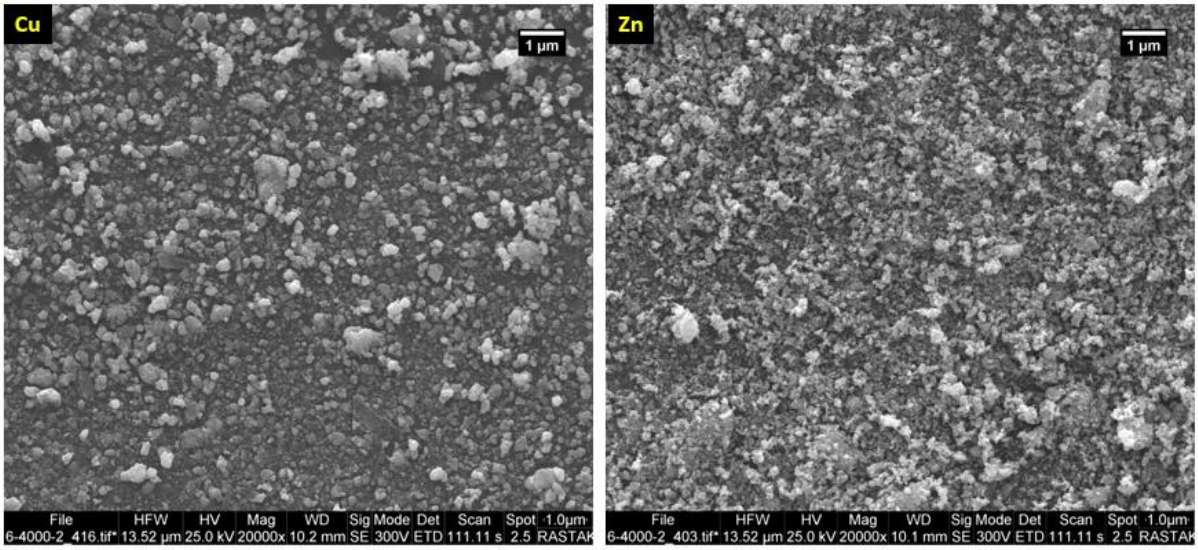


**Figure 4.** Scanning electron microscope image of Cu and Zn NPs synthesized by moringa plant aqueous extract.

To assess the purity of the produced NPs, the X-ray diffraction spectrum was examined, and elemental composition was confirmed through EDX analysis (Figure 5A). The EDX pattern verified the presence of biosynthesized elements, with copper ions at 60.99%, oxygen at 18.06%, aluminum at 10.55%, silicon at 7.03%, and iron at 3.37%—proportions consistent with those defined during synthesis (Figure 5A). The primary contaminants in the spectrum—oxygen, aluminum, silicon, and iron—are attributed to physical adsorption during sample preparation.

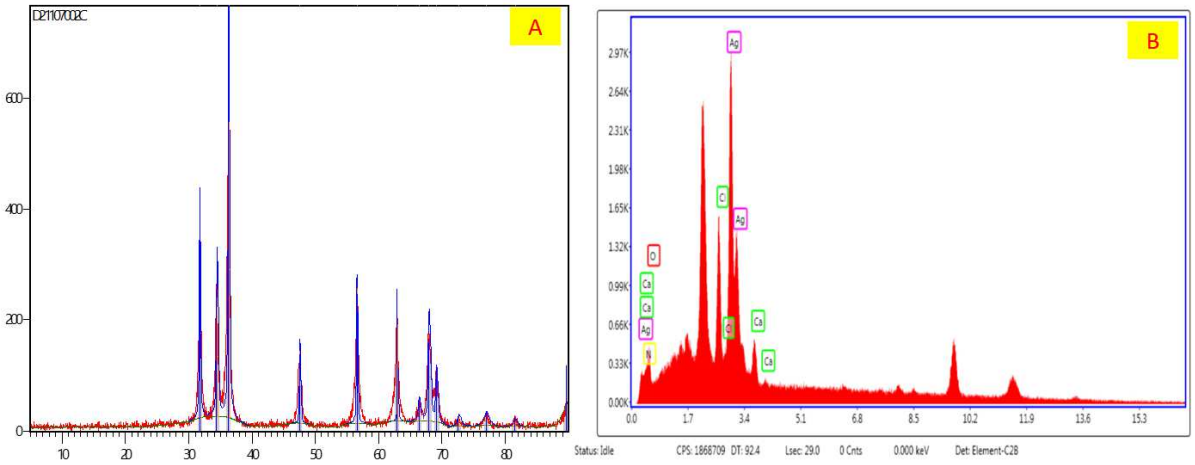


**Figure 5.** EDX spectrum of Cu NPs (A) and Zn NPs (B) synthesized by aqueous extract of moringa plant

To assess the purity of the produced Zn NPs, the X-ray diffraction spectrum was examined, and the presence of zinc metal was confirmed through EDX analysis (Figure 5B).

The presence of double peaks in the FTIR spectra (Figure 6) of Cu and Zn NPs in the 4000–3500 $cm^{-1}$ range corresponds to stretching vibrations of the O–H group. Double and elongated peaks in the 2800–3500 $cm^{-1}$ region indicate the presence of metal NPs. Furthermore, absorption peaks in the 500–1500 $cm^{-1}$ region were attributed to C=O, N–H, and O–C bonds. Since organic compounds from the plant extract surround the NPs and contribute to their stability, the vibrational modes of these functional groups are evident in the FTIR spectrum (Figure 6).

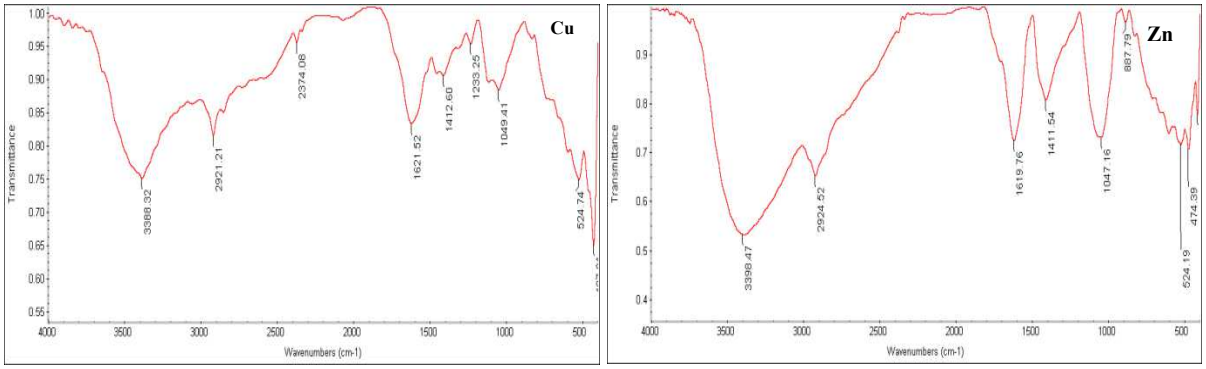


**Figure 6.** Fourier Transform Infrared Spectrometer (FTIR) spectrum of Cu and Zn NPs biosynthesized from aqueous extract of plant moringa

The XRD analysis was performed using a Cu anode ($K\alpha_1$ = 1.54060 Å, $K\alpha_2$ = 1.54443 Å) with a goniometer scan over a 2θ range of 5.0000° to 89.9600° at a step size of 0.0400° and a scan step time of 1.0000 s. A fixed divergence slit of 1.0000° and a receiving slit of 0.1000 mm were used, without an incident beam monochromator or sample spinning. The measurement was conducted at 25.00°C with a goniometer radius of 240.00 mm and a focus-divergence slit distance of 91.00 mm. The XRD peak list revealed distinct diffraction patterns with prominent peaks at 27.6894°, 32.0889°, 38.2331°, 46.4645°, and 76.9763° 2θ. The highest intensity peak (100% relative intensity) was at 32.0889° with a d-spacing of 2.789 Å, closely matching reference pattern 96-901-1667. Peaks at 27.6894° (55.92% intensity, d = 3.222 Å) and 46.4645° (58.72% intensity, d = 1.954 Å) also aligned with this reference, while the peak at 38.2331° (43.06% intensity, d = 2.354 Å) corresponded to phase 01-087-0720. The broad peak at 76.9763° (12.17% intensity, d = 1.239 Å) showed overlap with both reference patterns, indicating a possible mixed-phase composition. FWHM values suggested varying crystallite sizes, with the sharpest peak at 32.0889° (FWHM = 0.7872°). Overall, the results confirmed multiple crystalline phases, with 96-901-1667 as the dominant reference pattern (Figure 7).

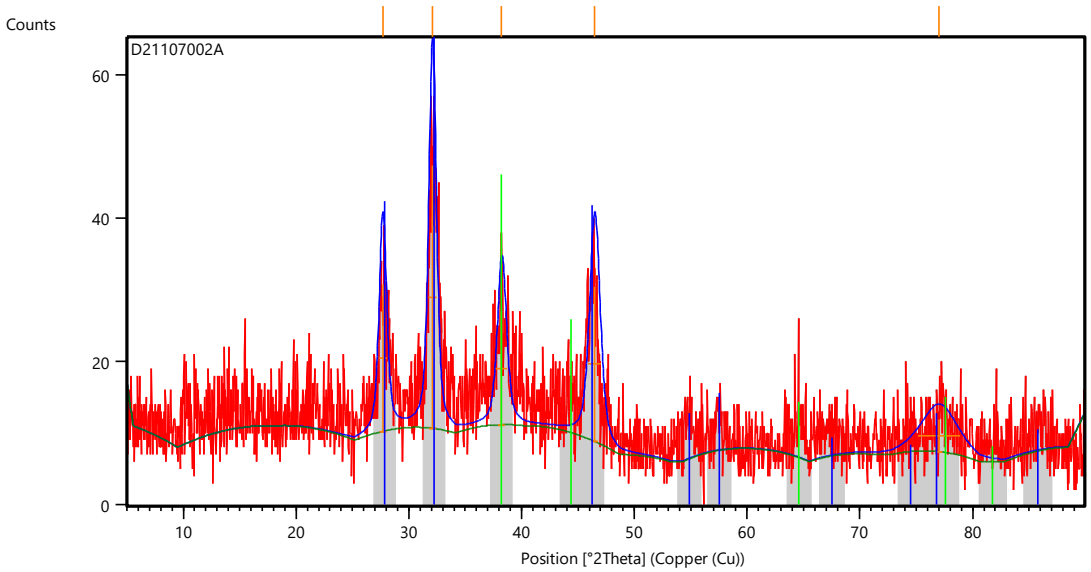


**Figure 7.** XRD Analysis Using Cu-Kα Radiation Reveals Dominant Crystalline Phase (96-901-1667) with Secondary Phase (01-087-0720) in Mixed Composition

**Callus induction in chicory plant**

As shown in Table 3, optimization of the callus induction environment (Figure 8) in MS medium supplemented with various concentrations of Cu NPs (0, 100, 150, and 200 mg/l) and Zn NPs (0, 100, 150, and 200 mg/l) revealed that the highest values for chlorophyll content, fresh weight, and dry weight of callus were obtained with 100 mg/L Cu NPs. This treatment resulted in a significant increase compared to the others. Additionally, the highest proline content was achieved with 150 mg/l Cu NPs, showing a 13.71% increase over the 200 mg/l treatment.

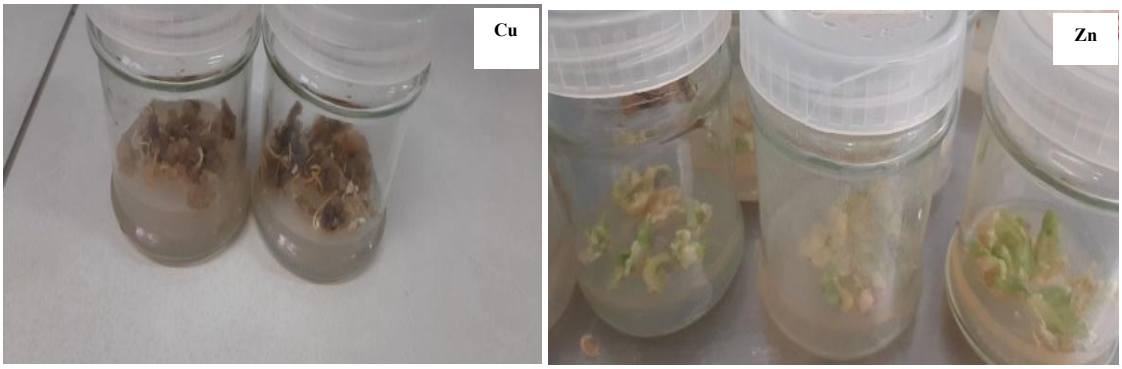


**Figure 8.** Induction of callus in a chicory plant under the influence of Cu and Zn NPs synthesized by aqueous extract of moringa plant.

**Descriptive statistical analysis**

Descriptive statistics, including mean, standard deviation, minimum, maximum, range, and coefficient of variation (CV) for the studied traits, are summarized in table 1. Among the CV values, carotenoids exhibited the highest (43.35%), while callus dry weight showed the lowest (0.51%). Table 1 indicates that total chlorophyll had the largest range of variation, though it did not correspond to the highest standard error. The results revealed substantial variation among treatments for carotenoids, chlorophyll a, and callus fresh weight.

**Table 1.** Descriptive statistics of studied traits of chicory during Cu NPs treatment

| Trait | Mean ± SE | PCV (%) | Minimum | Maximum | Range |
|---|---|---|---|---|---|
| Ch. a | 2.72±0.17 | 4.69 | 1.13 | 3.32 | 2.18 |
| Ch. b | 1.96±0.21 | 2.74 | 0.59 | 2.75 | 2.15 |
| Ch. T | 4.68±0.37 | 3.76 | 1.73 | 6.07 | 4.34 |
| Car | 2.77±0.01 | 43.35 | 2.62 | 2.86 | 0.24 |
| Proline | 0.20±0.02 | 2.37 | 0.12 | 0.37 | 0.25 |
| CFW | 0.64±0.04 | 3.97 | 0.34 | 0.82 | 0.47 |
| CDW | 0.11±0.06 | 0.51 | 0.01 | 0.78 | 0.76 |

Chlorophyll a (Ch. a): mg/g fresh weight (FW), Chlorophyll b (Ch. b): mg/g fresh weight (FW), Total Chlorophyll (Ch. T): mg/g fresh weight (FW), Carotenoids (Car): mg/g fresh weight (FW), Proline (Proline): µmol/g fresh weight (FW), Callus Fresh Weight (CFW): gram (g) and Callus Dry Weight (CDW): gram (g)

Descriptive statistics, including mean, standard deviation, minimum, maximum, range, and coefficient of variation (CV) for the studied traits, are summarized in table 2. Among the CV values, proline exhibited the highest (13.35%), while callus dry weight showed the lowest (1.10%). Table 2 indicates that total chlorophyll had the largest range of variation, though it did not correspond to the highest standard error. The results revealed substantial variation among treatments for proline, callus fresh weight, and carotenoids.

**Table 2.** Descriptive statistics of studied characteristics of chicory during Zn NPs treatment

| Trait | Mean ± SE | PCV (%) | Minimum | Maximum | Range |
|---|---|---|---|---|---|
| Ch. a | 1.38±0.33 | 1.25 | 0.04 | 2.97 | 2.93 |
| Ch. b | 0.91±0.24 | 1.13 | 0.13 | 2.32 | 2.19 |
| Ch. T | 2.29±0.56 | 1.22 | 0.32 | 5.30 | 4.98 |
| Car | 1.75±0.27 | 1.89 | 0.35 | 2.80 | 2.45 |
| Proline | 0.26±0.006 | 13.35 | 0.21 | 0.28 | 0.07 |
| CFW | 0.73±0.05 | 4.07 | 0.45 | 0.97 | 0.52 |
| CDW | 0.06±0.01 | 1.10 | 0.01 | 0.20 | 0.19 |

Chlorophyll a (Ch. a): mg/g fresh weight (FW), Chlorophyll b (Ch. b): mg/g fresh weight (FW), Total Chlorophyll (Ch. T): mg/g fresh weight (FW), Carotenoids (Car): mg/g fresh weight (FW), Proline (Proline): µmol/g fresh weight (FW), Callus Fresh Weight (CFW): gram (g) and Callus Dry Weight (CDW): gram (g)

**Mean comparison analysis**

Table 3 presents the mean growth characteristics of chicory plants under Cu and Zn NP treatments. Significant differences were observed among treatments. As shown in Table 3, the highest values for chlorophylls, callus fresh weight, and dry weight were obtained with 100 mg/L Cu NPs, showing a significant increase compared to other treatments. The highest proline content was achieved with 150 mg/l Cu NPs, representing increases of 13.71% over 200 mg/l, 120% over the control, and 106.25% over 100 mg/L. Chlorophyll a, b, and total chlorophyll were highest in the control treatment. The highest carotenoid content was observed with 100 mg/L Zn NPs. Additionally, proline (150 mg/L treatment) and callus fresh and dry weights (200 mg/L treatment) exhibited maximum values (Table 3).

**Table 3.** Comparison of the average characteristics of chicory under the treatment of Cu and Zn NPs

| | **Cu** | | | |
|---|---|---|---|---|
| | 0 mg/l | 100 mg/l | 150 mg/l | 200 mg/l |
| Ch. a | 2.90±0.0017$^{ab}$ | 3.15±0.0320$^{a}$ | 2.28±0.2936$^{c}$ | 2.61±0.0300$^{bc}$ |
| Ch. b | 2.59±0.0008$^{a}$ | 2.62±0.0804$^{a}$ | 1.49±0.4503$^{b}$ | 1.35±0.0574$^{b}$ |
| Ch. T | 5.49±0.0018$^{a}$ | 5.77±0.1089$^{a}$ | 3.78±0.6673$^{b}$ | 3.96±0.0875$^{b}$ |
| Car | 2.79±0.0263$^{ab}$ | 2.83±0.0203$^{a}$ | 2.71±0.0424$^{b}$ | 2.76±0.0064$^{ab}$ |
| Proline | 0.15±0.0038$^{b}$ | 0.16±0.0045$^{b}$ | 0.33±0.0289$^{a}$ | 0.14±0.0098$^{b}$ |
| CFW | 0.68±0.0302$^{b}$ | 0.80±0.0092$^{a}$ | 0.41±0.0355$^{c}$ | 0.67±0.0182$^{b}$ |
| CDW | 0.05±0.0012$^{b}$ | 0.31±0.0230$^{a}$ | 0.02±0.0054$^{b}$ | 0.04±0.0063$^{b}$ |
| | **Zn** | | | |
| | 0 mg/l | 100 mg/l | 150 mg/l | 200 mg/l |
| Ch. a | 2.92±0.0286$^{a}$ | 1.46±0.0191$^{b}$ | 0.25±0.0364$^{b}$ | 1.39±0.0757$^{b}$ |
| Ch. b | 2.30±0.0321$^{a}$ | 1.00±0.0117$^{b}$ | 0.15±0.0121$^{c}$ | 0.67±0.0355$^{bc}$ |
| Ch. T | 5.23±0.0581$^{a}$ | 2.460.0989$^{b}$ | 0.41±0.0477$^{c}$ | 2.06±0.0796$^{bc}$ |
| Car | 2.46±0.3209$^{a}$ | 2.55±0.0071$^{a}$ | 1.18±0.0885$^{b}$ | 1.16±0.0760$^{b}$ |
| Proline | 0.22±0.0240$^{b}$ | 0.26±0.0076$^{ab}$ | 0.28±0.0037$^{a}$ | 0.27±0.0003$^{a}$ |
| CFW | 0.79±0.0480$^{b}$ | 0.68±0.0269$^{c}$ | 0.51±0.0325$^{d}$ | 0.94±0.0150$^{a}$ |
| | 0.06±0.0030$^{b}$ | 0.03±0.0069$^{b}$ | 0.02±0.0069$^{b}$ | 0.15±0.0023$^{a}$ |

Chlorophyll a (Ch. a): mg/g fresh weight (FW), Chlorophyll b (Ch. b): mg/g fresh weight (FW), Total Chlorophyll (Ch. T): mg/g fresh weight (FW), Carotenoids (Car): mg/g fresh weight (FW), Proline (Proline): µmol/g fresh weight (FW), Callus Fresh Weight (CFW): gram (g) and Callus Dry Weight (CDW): gram (g)

**Correlation coefficient results**

The correlation matrix for growth characteristics under Cu NPs treatments (Figure 9) showed that increases in chlorophyll a were accompanied by increases in chlorophyll b and total chlorophyll. A positive relationship was also observed between carotenoids and chlorophyll b. Notably, proline exhibited significant positive correlations

with chlorophyll a (0.4671*), chlorophyll b (0.5768*), total chlorophyll (0.5406*), and carotenoids (0.7632*). This indicates that higher proline levels enhance chlorophyll synthesis. The correlation matrix for growth traits under Cu NPs treatments is presented in Figure 10.

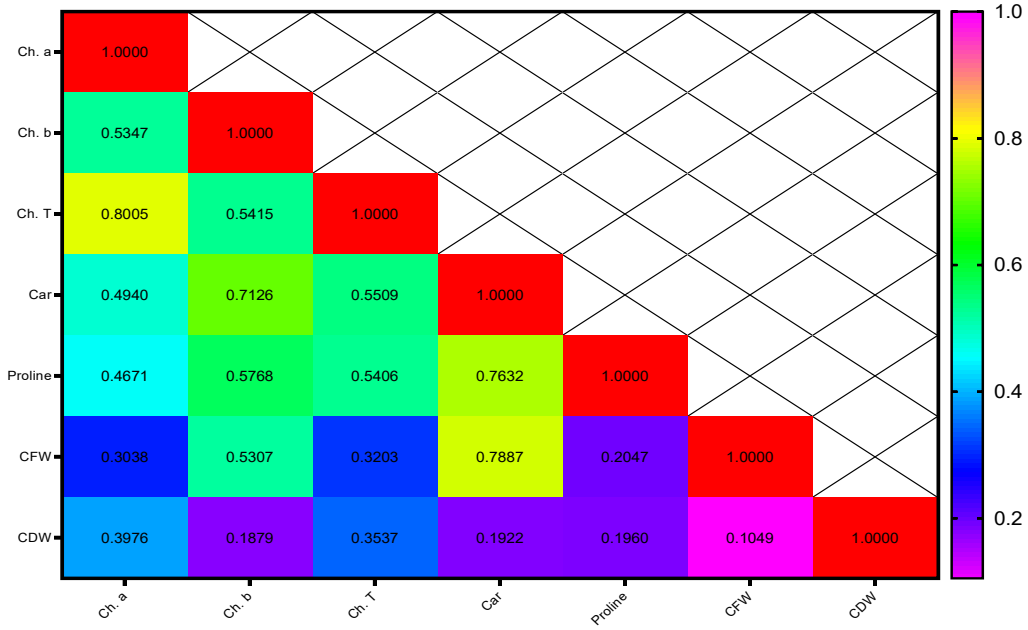


**Figure 9.** Heat map of mutual relations of variables in correlation coefficient for indicators under Zn NPs. Chlorophyll a (Ch. a): mg/g fresh weight (FW), Chlorophyll b (Ch. b): mg/g fresh weight (FW), Total Chlorophyll (Ch. T): mg/g fresh weight (FW), Carotenoids (Car): mg/g fresh weight (FW), Proline (Proline): µmol/g fresh weight (FW), Callus Fresh Weight (CFW): gram (g) and Callus Dry Weight (CDW): gram (g)

The correlation matrix for growth traits under Zn NPs treatments showed that increases in carotenoids and callus fresh weight were associated with exponential increases in chlorophylls. However, a significant negative relationship was observed between proline and the other traits (Figure 11).

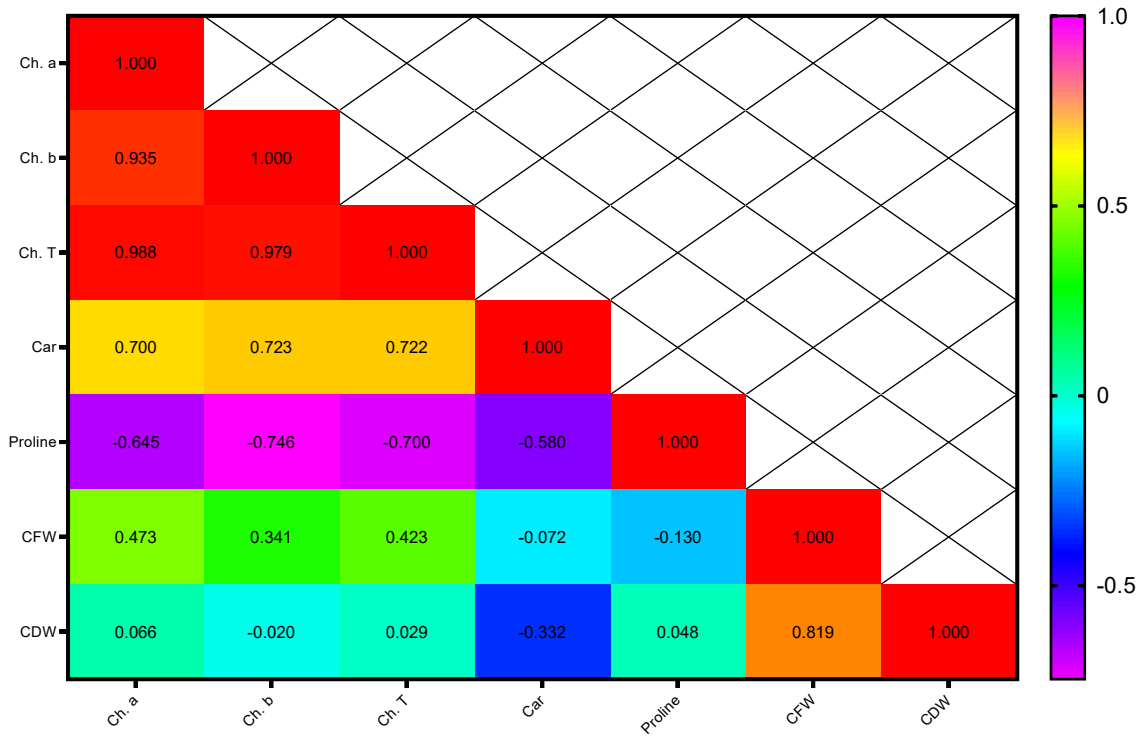


**Figure 10.** Heat map of mutual relations of variables in correlation coefficient for indicators under Cu NPs. Chlorophyll a (Ch. a): mg/g fresh weight (FW), Chlorophyll b (Ch. b): mg/g fresh weight (FW), Total Chlorophyll (Ch. T): mg/g fresh weight (FW), Carotenoids (Car): mg/g fresh weight (FW), Proline (Proline): µmol/g fresh weight (FW), Callus Fresh Weight (CFW): gram (g) and Callus Dry Weight (CDW): gram (g)

**Path analysis results**

Path analysis was employed to examine relationships between traits. This method partitions correlations between independent and dependent variables into direct and indirect effects, facilitating accurate result interpretation. High correlations between traits can cause multicollinearity, which distorts conventional Path analysis models and produces unrealistic estimates with high error. Sequential Path analysis, used in this study, reduces multicollinearity and simplifies trait relationships. Direct effects, total indirect effects of studied traits on callus dry weight, and correlations are presented in Table 4. Indirect effect analysis for Zn NPs treatments is shown in Figure 12**.**

Stepwise regression analysis results for Cu and Zn NPs treatments are shown in Table 4. Key traits identified in the models included: chlorophyll a (0.067 and -0.031), chlorophyll b (-0.0066 and 6.56), carotenoids (1.690 and 0.005), proline (1.817 and -0.304), and callus fresh weight (0.861 and 0.375), each contributing significantly to percentage changes in callus dry weight (Table 4).

**Table 4.** Step-by-step regression analysis of callus dry weight with other traits included in the model during the treatment of Cu and Zn NPs.

| **Variables entered to model** | **Step 1** | |
|---|---|---|
| | **Cu** | **Zn** |
| Intercept | -5.552 | -0.091 |
| Ch. a | 0.067 | -0.031 |
| Ch. b | -.0066 | 6.56 |
| Car | 1.690 | 0.005 |
| Proline | 1.817 | -0.304 |
| CFW | 0.861 | 0.375 |
| $R^2$ (%) | 0.362 | 0.819 |

The results from Cu and Zn NPs treatments showed that in the first stage of Path analysis, chlorophylls (a, b, and carotenoids), proline, and callus fresh weight had the greatest influence on determining callus dry weight. The highest positive direct effects were associated with proline (0.708) and callus fresh weight (1.091), while the lowest

direct effects were linked to chlorophyll b (−0.218) and chlorophyll a (−0.605), both of which were negative (Table 5).

**Table 5.** Direct analysis of callus dry weight with other traits entered into the model during the treatment of Cu and Zn NPs.

| | Ch. a | Ch. b | Car | Proline | CFW |
|---|---|---|---|---|---|
| Cu | 0.175 | -0.218 | 0.497 | 0.708 | 0.624 |
| Zn | -0.605 | 0.001 | 0.081 | -0.152 | 1.091 |

The results of indirect effect analysis for Cu and Zn NPs treatments are presented in figures 11 and 12. These findings indicate that the traits chlorophyll a (0.067 and −0.031, respectively), chlorophyll b (−0.0066 and 6.56), carotenoids (1.690 and 0.005), proline (1.817 and −0.304), and callus fresh weight (0.861 and 0.375) exerted primarily indirect effects on callus dry weight.

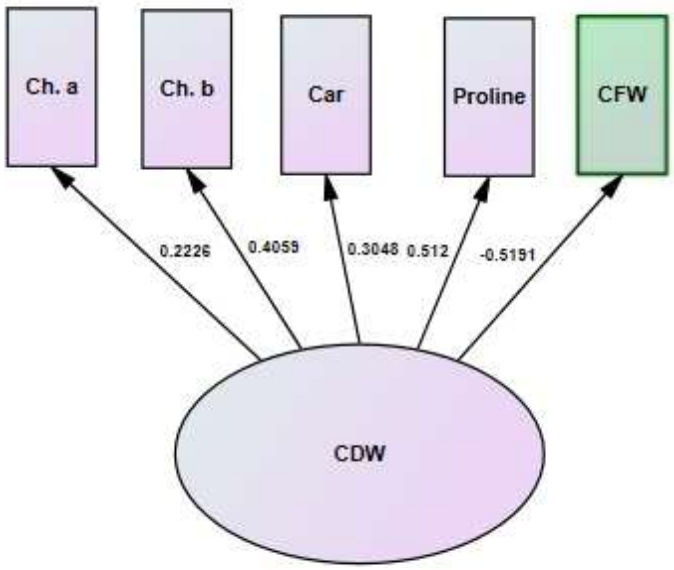


**Figure 11.** Indirect analysis of callus dry weight trait with other traits entered into the model during Cu NPs treatment.

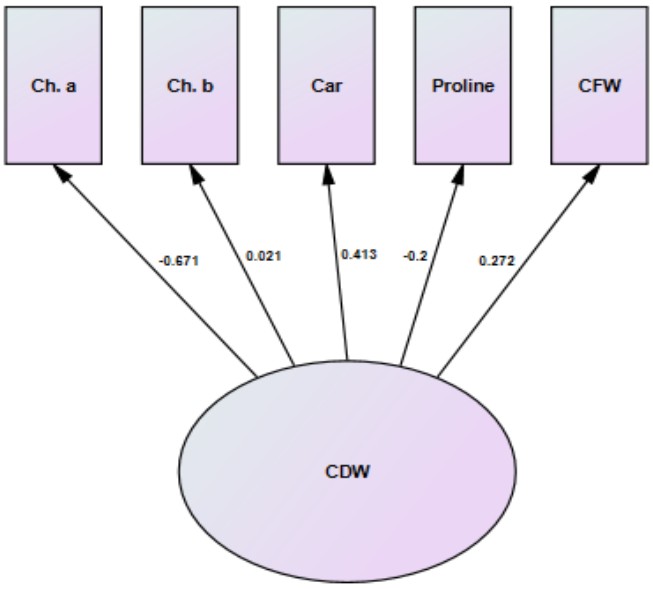


**Figure 12.** Indirect analysis of the callus dry weight attribute with other attributes entered into the model during the treatment of Zn NPs.

**Discussion**

The chicory plant is an important medicinal plant with valuable secondary metabolites (Koohsari et al. 2020; Janda et al. 2021). Chicory callus serves as an effective source for producing and extracting these metabolites. Advanced tissue culture techniques in breeding and propagating medicinal plants enable greater utilization and yield of valuable secondary compounds. Combining these methods with nanotechnology can enhance production efficiency (Rizwan et al. 2017).

Various NPs synthesis methods exist, but physical and chemical approaches often produce environmentally harmful byproducts and can be replaced by green synthesis, which uses less toxic materials (Patel et al. 2023). *Moringa* is a rich source of minerals, vitamins, proteins, and antioxidants (Adedapo et al. 2015), making it suitable for NPs production. Given the regional abundance of this tropical plant and its beneficial compounds, this study was conducted in October 2023 at the University of Zabol to optimize chicory callus production using Zn and Cu NPs synthesized from moringa aqueous extract. The results demonstrated that Moringa extract effectively produced Cu and Zn NPs. Since NPs size and shape are critical for medicinal applications, electron microscopy revealed average sizes of 8 nm for Cu NPs and 12 nm for Zn NPs, all spherical. The homogeneous spherical morphology observed via SEM and TEM indicates successful capping by bioactive molecules from moringa extract. Different concentrations (0, 100, 150, and 200 mg/L) of Cu and Zn NPs synthesized from moringa aqueous extract were tested on chlorophyll a, b, total chlorophyll, carotenoids, and proline in chicory. The maximum effects of Cu NPs on chlorophylls, callus fresh weight, and dry weight were observed at 100 mg/L, showing significant increases over other treatments. The highest proline content was obtained at 150 mg/L Cu NPs, representing increases of 13.71% over 200 mg/L, 120% over control, and 106.25% over 100 mg/L. However, Cu NPs concentrations above 100 mg/L reduced chlorophyll a, b, total chlorophyll, carotenoids, and proline.

The mechanism by which NPs enhance growth is not fully elucidated, but improved water uptake may be a primary factor. NPs penetrate cell walls and membranes, forming new pores that facilitate water and mineral influx (Tiwari et al. 2014). Increased water uptake raises turgor pressure, alters cellular osmotic potential, and enhances mineral absorption. This triggers enzymatic and hormonal signaling, boosting growth enzyme activity and levels of gibberellins and auxins, promoting tissue expansion (Taiz and Zeiger 2002). Research suggests NPs influence hormone distribution and microtubule organization to accelerate cell division and growth (Liu et al. 2009). Nanomaterials may also enter cells via aquaporins, ion channels, or new pores, modulating gene expression and metabolic pathways to improve efficiency, growth, and quality in various plants (Aslani et al. 2014). Copper is essential for plant growth, forming part of protein structures and required by over 30 enzymes, including superoxide dismutase (SOD) and cytochrome c oxidase. It supports photosynthesis, protein, and carbohydrate metabolism, but excess copper causes toxicity and growth inhibition (Adrees et al. 2015; Ngo et al. 2014; Pirooz et al. 2022; Yasmeen et al. 2017; Hernández-Hernández et al. 2019; Nazir et al. 2021; Lafmejani et al. 2018). High intracellular copper disrupts photosynthesis, induces metabolic disorders, and generates oxidative stress (Adrees et al. 2015). Like copper ions, Cu NPs exhibit both positive and negative effects. CuO NPs have been reported to enhance soybean yield (Ngo et al. 2014), stimulate phenolic production in sage (Pirooz et al. 2022), increase wheat yield under drought (Yasmeen et al. 2017), promote active compound accumulation in tomato fruit (Hernández-Hernández et al. 2019), boost phenolics and flavonoids in basil (Nazir et al. 2021), and increase essential oil in

peppermint (Lafmejani et al. 2018). Conversely, high CuO NPs concentrations reduce photosynthetic pigments in *Arabidopsis* (Nair et al. 2022) and elevate malondialdehyde and Cu-Zn SOD gene expression in cucumber (Mosa et al. 2018).

Our results show that Cu NPs concentrations above 100 mg/L decreased chlorophyll, carotenoids, and callus fresh and dry weights, likely due to copper ion release affecting callus growth and chlorophyll synthesis. Copper is vital for chlorophyll formation, photosynthesis, carbohydrate and nitrogen metabolism, and enzyme activation (Krzepiłko et al. 2024). It promotes cell elongation by influencing nitrogen metabolism, tryptophan synthesis, and auxin production (Adrees et al. 2015). However, high copper release at elevated Cu NPs levels damages chromatin, increases membrane lipid peroxidation, degrades chlorophyll, and impairs photosynthesis, ultimately reducing growth and potentially causing plant death (Kasana et al. 2017).

Zinc is a limiting but essential element, incorporated into over 200 enzymes and involved in hormone synthesis (Taiz and Zeiger 2002). High concentrations inhibit growth (Paschke et al. 2006). Nano-ZnO at 100 ppm maximized callus induction and survival in *Hypericum perforatum* (Mezginezhad et al. 2019), while ZnO NP toxicity reduced root fresh weight in fenugreek (Fallah 2017). In this study, Zn NPs from moringa extract yielded the highest carotenoid content at 100 mg/L, with maximum proline at 150 mg/L and callus fresh and dry weights at 200 mg/L. Overall, Cu and Zn NPs treatments showed the strongest positive direct effects on proline (0.708) and callus fresh weight (1.091), while the weakest, negative effects were on chlorophyll b (−0.218) and chlorophyll a (−0.605).

Carotenoids, tetraterpene compounds, protect chlorophyll from photooxidation, absorb light, and transfer energy to chlorophyll (Devlin and Witham 2001). They act as non-photosynthetic pigment supporters, quenching excess short-wavelength energy, converting singlet to triplet oxygen, and scavenging radicals to exert antioxidant effects (Inzé and Van Montagu 1995). Proline, the most stable amino acid, confers oxidative stress resistance by enhancing antioxidant enzyme activity, neutralizing reactive oxygen species (ROS), and maintaining redox balance (Sharma et al. 2011). Proline levels in wheat increased significantly with NPs concentration, peaking at 100 mg/L, consistent with our findings (Karimi and Mohsenzadeh 2017). Proline thus serves as a defense against oxidative stress. Zinc concentration increases proline accumulation, which mitigates environmental stress, including heavy metals, in plants and microorganisms (Siripornadulsil et al. 2002). Stress-induced proline accumulation reduces membrane and protein damage (Matysik et al. 2002). Proline synthesis lowers cytoplasmic osmotic potential, maintains the $NADP^+$/NADPH ratio, and functions as an osmolyte, radical scavenger, macromolecule stabilizer, and cell wall component (Llamas et al. 2000). Under heavy metal stress, glutamate shifts from chlorophyll to proline synthesis to protect against toxicity. In this study, proline levels in chicory increased with higher zinc and copper nanooxide concentrations (Vankhadeh 2002).

Zn NPs treatments increased leaf chlorophyll and plant dry weight (Vankhadeh 2002). The rise in photosynthetic pigments and carotenoids under nano-ZnO suggests a protective role against xenobiotic production in tissue culture. Thus, 100 mg/L nano-ZnO in chicory medium can enhance total chlorophyll and carotenoids. Nano-ZnO also improves elemental uptake, increasing plant zinc content (Zeyaeyan and Malakote 2000). Zn NPs positively affect growth in banana (Helaly et al. 2014), chickpea (Helaly et al. 2014), peanut (Singh et al. 2015), onion and soybean (Khot et al. 2012). In banana tissue culture, maximum growth occurred at 100 mg/L Zn NPs, aligning with our results (Helaly et al. 2014). ZnO NPs significantly boosted growth and yield in pea, peanut, and millet (Singh et al. 2015). In our study, 100 mg/L ZnO NPs likely improved chicory tissue culture conditions, increasing photosynthetic pigments. Optimal NPs concentrations vary by plant species, NPs type, dose, application method, duration, and species (Ma et al. 2015), consistent with prior reports.

Previous studies indicate that NPs concentrations of silver, copper, copper oxide, titanium dioxide, zinc, and zinc oxide disrupt growth in cucumber, lettuce, beans, corn, rye, and zucchini (Zhang et al. 2011). At toxic levels, plants reduce NPs uptake or toxicity. NPs toxicity correlates with plant species, with mung bean sprouts more sensitive than wheat (Lee et al. 2008). NPs may impair water and mineral transport and disrupt photosynthesis (Asli and Neumann 2009). Chlorophyll is critical for plant growth, with biosynthesis and degradation regulated by complex pathways. Callus fresh and dry weights, increased by zinc and copper oxide NPs in chicory, are key indicators of callus growth and health, potentially enhancing secondary metabolite production (Parabia et al. 2007; Dekami et al. 2023).

Recent studies highlight plants as eco-friendly sources for biocompatible NPs. Gold NP synthesis was optimized using moringa extract. Plant powder was heated to 30°C, mixed with $HAuCl_4 \cdot 3H_2O$, reducing gold ions to NPs and turning the solution purple. Parameters (pH, extract volume, gold salt concentration, temperature, reaction time) were optimized via UV-Vis (peak at 550 nm). Spherical NPs (10–40 nm) showed moderate antimicrobial activity against four pathogens, suggesting biomedical potential (Azizian-Shermeh et al. 2025). NPs from moringa extract exhibit significant biological potential. With further studies on side effects and optimization, they could be applied in food, pharmaceutical, and agricultural industries. However, most NP studies focus on germination; ecological toxicity, environmental risk to organisms across trophic levels, and bioavailability/bioaccumulation via food chains require urgent investigation

## Conclusion

The results of using Cu and Zn NPs synthesized from moringa plant aqueous extract on chicory callus formation showed that the strongest positive direct effects were on proline and callus fresh weight, while the weakest direct effects, which were negative, were on chlorophyll b and a. Therefore, based on the present study, the regional moringa plant aqueous extract effectively produces Cu and Zn NPs, which at low concentrations enhance callus formation and photosynthetic pigments in chicory in vitro. Specifically, 100 mg/L of Zn and CuO NPs improved chicory callus formation by increasing callus fresh and dry weights and photosynthetic pigments. Zn and Cu NPs promote cell growth, elongation, and metabolic rates by enhancing water and nutrient absorption. However, at higher concentrations, these effects reverse due to the toxicity of these elements, arising from their redox properties. Electron microscopy confirmed that the synthesized NPs were spherical, with average sizes of 8 nm for Cu NPs and 12 nm for Zn NPs. Consequently, this research indicates that the beneficial effects of NPs on plant growth can be harnessed for molecular studies and plant biotechnology applications to optimize growth.

## Declarations

### Ethics approval and consent to participate

All methods performed in this study including the collection of plant materials were in compliance with the relevant institutional, national, and international guidelines and legislation.

### Consent for publication

Not applicable

### Data Availability

The raw data of this article will be made available by corresponding author according to the personal requests.

### Conflict of interest

The authors declare no competing interests.

### Funding

Not applicable

### Authors' contribution statement

**Hamideh Khajeh** and **Bahman Fazeli-Nasab**: Conceptualization, Methodology, Software, Validation, Visualization, Writing- Original Draft. **Ali Salehi Sardoei**: Formal Analysis, Investigation, Resources, Data curation. **Zeinab Fotoohiyan**: Writing - Original Draft and Revision. **Ali Reza Mirzaei**: Supervision, Project administration, Software, Writing - Original Draft and Revision. **Mohammad Reza Asgharipour**: Writing - Review and preparation of final version. All authors have read and agreed to the published version of the manuscript.

## References

Abhilash A, Dayal A, Thomas N, Sharan A, Vipul V (2023) Effect of zinc oxide (ZnO) nanoparticles on the storability of onion (*Allium cepa* L.) seeds under ambient condition. Int J Plant Soil Sci 35:455–468. https://doi.org/10.9734/ijpss/2023/v35i184555

Adedapo AA, Falayi OO, Oyagbemi AA (2015) Evaluation of the analgesic, anti-inflammatory, anti-oxidant, phytochemical and toxicological properties of the methanolic leaf extract of commercially processed *Moringa oleifera* in some laboratory animals. J Basic Clin Physiol Pharmacol 26:491–499. https://doi.org/10.1515/jbcpp-2014-0101

Adrees M, Ali S, Rizwan M, Ibrahim M, Abbas F, Farid M, Zia-ur-Rehman M, Irshad MK, Bharwana SA (2015) The effect of excess copper on growth and physiology of important food crops: a review. Environ Sci Pollut Res 22:8148–8162. https://doi.org/10.1007/s11356-015-4197-5

Ahmad MA, Javed R, Adeel M, Rizwan M, Yang Y (2020) Engineered ZnO and CuO nanoparticles ameliorate morphological and biochemical response in tissue culture regenerants of candyleaf (*Stevia rebaudiana*). Molecules 25:1356. https://doi.org/10.3390/molecules25061356

Ahmed R, Yusuf M, Khan S, Naseem S, Ali S, Javed M, Ahmad S, Zubair M, Ahmad P (2023) Impact of foliar application of zinc and zinc oxide nanoparticles on growth, yield, nutrient uptake and quality of tomato. Horticulturae 9:162. https://doi.org/10.3390/horticulturae9020162

Alavi M, Hamblin MR (2023) Antibacterial silver nanoparticles: effects on bacterial nucleic acids. Cell Mol Biomed Rep 3:35–41. https://doi.org/10.55705/cmbr.2023.376543.1095

Alavi M, Hamblin MR, Mozafari MR, Rose Alencar de Menezes I, Douglas Melo Coutinho H (2022a) Surface modification of $SiO_2$ nanoparticles for bacterial decontaminations of blood products. Cell Mol Biomed Rep 2:87–98. https://doi.org/10.55705/cmbr.2022.345897.1044

Alavi M, Nokhodchi A, Alavi M, Hamblin MR, Rose Alencar de Menezes I, Douglas Melo Coutinho H (2022b) The efficiency of metal, metal oxide, and metalloid nanoparticles against cancer cells and bacterial pathogens: different mechanisms of action. Cell Mol Biomed Rep 2:10–21. https://doi.org/10.55705/cmbr.2022.336404.1026

Aslani F, Bagheri S, Muhd Julkapli N, Juraimi AS, Hashemi FSG, Baghdadi A (2014) Effects of engineered nanomaterials on plants growth: an overview. ScientificWorldJournal 2014:641759. https://doi.org/10.1155/2014/641759

Azim Z, Singh A, Kumar A, Singh R, Singh PK, Kumar A (2023) A review summarizing uptake, translocation and accumulation of nanoparticles within the plants: current status and future prospectus. J Plant Biochem Biotechnol 32:211–224. https://doi.org/10.1007/s13562-022-00791-3

Azizian-Shermeh O, Kaedi F, Taherizadeh M, Qasemi A (2025) Convenient and cost-effective plant-mediated synthesis of gold nanoparticles using *Moringa oleifera* L. and study of their antimicrobial activities. Colloid Nanosci J 2:397–408. https://doi.org/10.61186/cnj.2.4.397

Barnes JD, Balaguer L, Manrique E, Elvira S, Davison AW (1992) A reappraisal of the use of DMSO for the extraction and determination of chlorophylls a and b in lichens and higher plants. Environ Exp Bot 32:85–100. https://doi.org/10.1016/0098-8472(92)90034-Y

Baskar V, Nayeem S, Kuppuraj SP, Muthu T, Ramalingam S (2018) Assessment of the effects of metal oxide nanoparticles on the growth, physiology and metabolic responses in in vitro grown eggplant (*Solanum melongena*). 3 Biotech 8:362. https://doi.org/10.1007/s13205-018-1398-3

Cai Y, Li X, Li X, Zhang Y, Wang X, Wang X, Li X (2022) Foliar application of $SiO_2$ and ZnO nanoparticles affected polycyclic aromatic hydrocarbons uptake of amaranth (*Amaranthus tricolor* L.): a metabolomics and typical statistical analysis. Sci Total Environ 833:155258. https://doi.org/10.1016/j.scitotenv.2022.155258

Chung IM, Rajakumar G, Subramanian U, Venkidasamy B, Thiruvengadam M (2019) Impact of copper oxide nanoparticles on enhancement of bioactive compounds using cell suspension cultures of *Gymnema sylvestre* (Retz.) R. Br. Appl Sci 9:2165. https://doi.org/10.3390/app9112165

Das S, Vasudeva N, Sharma S (2016) *Cichorium intybus*: a concise report on its ethnomedicinal, botanical, and phytopharmacological aspects. Drug Dev Ther 7:1–1. https://doi.org/10.4103/2394-2002.182821

Dekami A, Sanjarian F, Chaichi M, Hosseini B, Rahnama H (2023) Effect of plant growth regulators and light on callus induction, antioxidant enzyme response and total phenol in *Nigella arvensis* L. J Med Plants By-Prod 12:47–56. https://doi.org/10.30495/jmpb.2023.1971568.1602

Devlin R, Witham F (2001) *Plant Physiology*. CBS Publishers and Distributors, New Delhi, India

Fallah S (2017) Comparison between toxicity effects of ZnO nanoparticles and their bulk on fenugreek (*Trigonella foenum-graecum*) growth under greenhouse environment. J Plant Prod Res 24:23–42

Feng Y, Cui X, He S, Dong G, Chen M, Wang J, Lin X (2022) Effects of iron oxide nanoparticles ($Fe_3O_4$) on growth, photosynthesis, antioxidant activity and distribution of mineral elements in wheat (*Triticum aestivum*) plants. Plants 11:1894. https://doi.org/10.3390/plants11141894

Ghani MI, Saleem S, Raza A, Haider MZ, Ashfaq M, Saleem MH, Ali S (2022) Foliar application of zinc oxide nanoparticles: an effective strategy to mitigate drought stress in cucumber seedling by modulating antioxidant defense system and osmolytes accumulation. Chemosphere 289:133202. https://doi.org/10.1016/j.chemosphere.2021.133202

Ghorbanpour M, Mohammadi M, Kariman K (2021) Insights into nanoparticle-induced changes in plant photosynthesis. Photosynthetica 59:570–586. https://doi.org/10.1007/s11099-021-01259-1

Helaly MN, El-Metwally MA, El-Hoseiny H, Omar SA, El-Sheery NI (2014) Effect of nanoparticles on biological contamination of in vitro cultures and organogenic regeneration of banana. Aust J Crop Sci 8:612–624

Hernández-Hernández H, Quiterio-Gutiérrez T, Cadenas-Pliego G, Ortega-Ortiz H, Hernández-Fuentes AD, de la Fuente MC, Valdés-Reyna J, Juárez-Maldonado A (2019) Impact of selenium and copper nanoparticles on yield, antioxidant system, and fruit quality of tomato plants. Plants 8:355. https://doi.org/10.3390/plants8100355

Huang Y, Zhao L, Keller AA (2019) Antioxidant response of cucumber (*Cucumis sativus*) exposed to nano copper pesticide: quantitative determination via LC-MS/MS. Food Chem 270:47–52. https://doi.org/10.1016/j.foodchem.2018.07.069

Inzé D, Van Montagu M (1995) Oxidative stress in plants. Curr Opin Biotechnol 6:153–158. https://doi.org/10.1016/0958-1669(95)80024-7

Iziy E, Majd A, Vaezi-Kakhki MR, Nejadsattari T, Noureini SK (2019) Effects of zinc oxide nanoparticles on enzymatic and nonenzymatic antioxidant content, germination, and biochemical and ultrastructural cell characteristics of *Portulaca oleracea* L. Acta Soc Bot Pol 88:3639. https://doi.org/10.5586/asbp.3639

Janda K, Gutowska I, Geszke-Moritz M, Jakubczyk K (2021) The common cichory (*Cichorium intybus* L.) as a source of extracts with health-promoting properties—a review. Molecules 26:1814. https://doi.org/10.3390/molecules26061814

Javed R, Yucesan B, Zia M, Gurel E (2018) Elicitation of secondary metabolites in callus cultures of *Stevia rebaudiana* Bertoni grown under ZnO and CuO nanoparticles stress. Sugar Tech 20:194–201. https://doi.org/10.1007/s12355-017-0538-9

Kalisz A, Pokluda R, Jezdinský A, Sękara A, Kopeć A, Grabowska A, Kunicki E, Neugebauerová J, Šlosár M, Hrabovská K (2021) Nanoparticles of cerium, iron, and silicon oxides change the metabolism of phenols and

flavonoids in butterhead lettuce and sweet pepper seedlings. Environ Sci Nano 8:1945–1959. https://doi.org/10.1039/D1EN00146A
Karimi J, Mohsenzadeh S (2017) Physiological effects of silver nanoparticles and silver nitrate toxicity in *Triticum aestivum*. Iran J Sci Technol Trans A Sci 41:111–120. https://doi.org/10.1007/s40995-016-0139-1
Karimzadeh F, Haddad R, Garoosi G, Khademian R (2019) Effects of nanoparticles on activity of lignan biosynthesis enzymes in cell suspension culture of *Linum usitatissimum* L. Russ J Plant Physiol 66:756–762. https://doi.org/10.1134/S102144371905007X
Kasana RC, Panwar NR, Kaul RK, Kumar P (2017) Biosynthesis and effects of copper nanoparticles on plants. Environ Chem Lett 15:233–240. https://doi.org/10.1007/s10311-017-0615-5
Khajeh H, Nasab BF, Mirzaei AR, Farzanfar H (2023) Biosynthesis of zinc nanoparticles of *Capparis spinosa* plant extract and its investigation on morphophysiological properties of the *Moringa olifera* plant. J Med Bacteriol 11:17–29
Khot LR, Sankaran S, Maja JM, Ehsani R, Schuster EW (2012) Applications of nanomaterials in agricultural production and crop protection: a review. Crop Prot 35:64–70. https://doi.org/10.1016/j.cropro.2012.01.007
Koohsari A, Chaloui V, Akbarpour V (2020) Effect of explant type and growth regulators on callus formation and chicory secondary metabolites (*Cichorium intybus* L.). J Plant Prod Res 27:32–36
Krzepiłko A, Prażak R, Matyszczuk K (2024) Influence of zinc oxide nanoparticles in in vitro culture and bacteria *Bacillus thuringiensis* in ex vitro conditions on the growth and development of blackberry (*Rubus fruticosus* L.). Appl Sci 14:3743. https://doi.org/10.3390/app14093743
Kumar SS, Venkateswarlu P, Rao VR, Rao GN (2013) Synthesis, characterization and optical properties of zinc oxide nanoparticles. Int Nano Lett 3:30. https://doi.org/10.1186/2228-5326-3-30
Lafmejani ZN, Jafari AA, Moradi P, Moghadam AL (2018) Impact of foliar application of copper sulphate and copper nanoparticles on some morpho-physiological traits and essential oil composition of peppermint (*Mentha piperita* L.). Herba Pol 64:13–24. https://doi.org/10.2478/hepo-2018-0013
Largia MJV, Shilpha J, Satish L, Swamy MK, Ramesh M (2022) Phytochemical genomics: plant metabolomics and medicinal plant genomics. In: Swamy MK, Kumar A (eds) Phytochemical Genomics. Springer Nature Singapore, Singapore, pp 477–497. https://doi.org/10.1007/978-981-19-5779-6_20
Lee WM, An YJ, Yoon H, Kweon HS (2008) Toxicity and bioavailability of copper nanoparticles to the terrestrial plants mung bean (*Phaseolus radiatus*) and wheat (*Triticum aestivum*): plant agar test for water-insoluble nanoparticles. Environ Toxicol Chem 27:1915–1921. https://doi.org/10.1897/07-481.1
Llamas A, Ullrich CI, Sanz A (2000) $Cd^{2+}$ effects on transmembrane electrical potential difference, respiration and membrane permeability of rice (*Oryza sativa* L.) roots. Plant Soil 219:21–28. https://doi.org/10.1023/A:100477170
Ma C, White JC, Dhankher OP, Xing B (2015) Reduced silver nanoparticle phytotoxicity in *Crambe abyssinica* with enhanced glutathione production by overexpressing bacterial γ-glutamylcysteine synthase. Environ Sci Technol 49:10117–10126. https://doi.org/10.1021/acs.est.5b01703
Matysik J, Alia, Bhalu B, Mohanty P (2002) Molecular mechanisms of quenching of reactive oxygen species by proline under stress in plants. Curr Sci 82:525–532
Mezginezhad Z, Ghaderi M, Alizde Z, Izanloo A (2019) Effect of iron oxide and zinc oxide nanoparticles on callus viability of seedless barberry. J Crop Breed 11:198–205
Mosa KA, El-Naggar M, Ramamoorthy K, Alawadhi H, Elnaggar A, Alawadhi F, Al-Malki F, Alqurashi M, Al-Mushhin N, Al-Hazmi N, Al-Zahrani HS, Al-Qahtani WH, Alqahtani M, Alghamdi J, Alqahtani M, Alqahtani M (2018) Copper nanoparticles induced genotoxicity, oxidative stress, and changes in superoxide dismutase (SOD) gene expression in cucumber (*Cucumis sativus*) plants. Front Plant Sci 9:872. https://doi.org/10.3389/fpls.2018.00872
Nair GM, Sajini T, Mathew B (2022) Advanced green approaches for metal and metal oxide nanoparticles synthesis and their environmental applications. Talanta Open 5:100080. https://doi.org/10.1016/j.talo.2022.100080
Nazir S, Wani AB, Malik MA, Wani AH, Ganie SA, Zahid M, Lone R, Masoodi KZ, Khan SA, Khan F (2021) Copper oxide (CuO) and manganese oxide (MnO) nanoparticles induced biomass accumulation, antioxidants biosynthesis and abiotic elicitation of bioactive compounds in callus cultures of *Ocimum basilicum* (Thai basil). Artif Cells Nanomed Biotechnol 49:625–633. https://doi.org/10.1080/21691401.2021.1981807
Ngo QB, Dao TH, Nguyen HC, Tran DX (2014) Effects of nanocrystalline powders (Fe, Co and Cu) on the germination, growth, crop yield and product quality of soybean (Vietnamese species DT-51). Adv Nat Sci Nanosci Nanotechnol 5:015016. https://doi.org/10.1088/2043-6262/5/1/015016
Nikbakht M, Pour Ali P (2015) Biological production and antibacterial effect of synthesized Ag with aqua extract and methanol. Med Sci J Islam Azad Uni 12:112–118
Parabia FM, Gami B, Kothari I, Mohan J, Parabia M (2007) Effect of plant growth regulators on in vitro morphogenesis of *Leptadenia reticulata* (Retz.) W. & A. from nodal explants. Curr Sci 92:1290–1293

628 Paschke MW, Perry LG, Redente EF (2006) Zinc toxicity thresholds for reclamation forb species. Water Air Soil
629 Pollut 170:317–330. https://doi.org/10.1007/s11270-006-3092-9
630 Patel RR, Singh SK, Singh M (2023) Green synthesis of silver nanoparticles: methods, biological applications,
631 delivery and toxicity. Mater Adv 4:1831–1849. https://doi.org/10.1039/D3MA00028K
632 Pirooz P, Amooaghaie R, Ahadi A, Sharififar F, Torkzadeh-Mahani M (2022) Silicon and nitric oxide
633 synergistically modulate the production of essential oil and rosmarinic acid in *Salvia officinalis* under Cu stress.
634 Protoplasma 259:905–916. https://doi.org/10.1007/s00709-021-01703-5
635 Rizwan M, Ali S, Qayyum MF, Ok YS, Adrees M, Ibrahim M, Zia-ur-Rehman M, Farid M, Abbas lanzar F (2017)
636 Effect of metal and metal oxide nanoparticles on growth and physiology of globally important food crops: a critical
637 review. J Hazard Mater 322:2–16. https://doi.org/10.1016/j.jhazmat.2016.05.061
638 Roy K, Mao HQ, Huang SK, Leong KW (1999) Oral gene delivery with chitosan–DNA nanoparticles generates
639 immunologic protection in a murine model of peanut allergy. Nat Med 5:387–391. https://doi.org/10.1038/7391
640 Sena F, Monza J, Signorelli S (2024) Proline content determination in plant tissues. In: Corpas FJ, Palma JM (eds)
641 ROS Signaling in Plants: Methods and Protocols. Springer US, New York, NY, pp 183–194.
642 https://doi.org/10.1007/978-1-0716-3469-9_14
643 Sharma S, Villamor JG, Verslues PE (2011) Essential role of tissue-specific proline synthesis and catabolism in
644 growth and redox balance at low water potential. Plant Physiol 157:292–304.
645 https://doi.org/10.1104/pp.111.183210
646 Singh A, Singh NB, Hussain I, Singh H, Singh S (2015) Plant-nanoparticle interaction: an approach to improve
647 agricultural practices and plant productivity. Int J Pharm Sci Invent 4:25–40
648 Singh R, Chahal KK (2018) *Cichorium intybus* L: a review on phytochemistry and pharmacology. Int J Chem Stud
649 6:1272–1280
650 Siripornadulsil S, Traina S, Verma DPS, Sayre RT (2002) Molecular mechanisms of proline-mediated tolerance
651 to toxic heavy metals in transgenic microalgae. Plant Cell 14:2837–2847. https://doi.org/10.1105/tpc.004853
652 Street RA, Sidana J, Prinsloo G (2013) *Cichorium intybus*: traditional uses, phytochemistry, pharmacology, and
653 toxicology. Evid Based Complement Alternat Med 2013:579319. https://doi.org/10.1155/2013/579319
654 Tahvilian R, Zangeneh MM, Falahi H, Sadrjavadi K, Jalalvand AR, Zangeneh A (2019) Green synthesis and
655 chemical characterization of copper nanoparticles using *Allium saralicum* leaves and assessment of their
656 cytotoxicity, antioxidant, antimicrobial, and cutaneous wound healing properties. Appl Organomet Chem
657 33:e5234. https://doi.org/10.1002/aoc.5234
658 Taiz L, Zeiger E (2002) *Plant Physiology*, 3rd edn. Sinauer Associates, Inc., Publishers, Sunderland, MA
659 Tiwari DK, Dasgupta-Schubert N, Villaseñor Cendejas LM, Villegas J, Carreto Montoya L, Borjas García SE
660 (2014) Interfacing carbon nanotubes (CNT) with plants: enhancement of growth, water and ionic nutrient uptake
661 in maize (*Zea mays*) and implications for nanoagriculture. Appl Nanosci 4:577–591.
662 https://doi.org/10.1007/s13204-013-0237-3
663 Vankhadeh S (2002) Response of sunflower to applied Zn, Fe, P, N. nes S zz 1:143–145
664 Yasmeen F, Raja NI, Razzaq A, Komatsu S (2017) Proteomic and physiological analyses of wheat seeds exposed
665 to copper and iron nanoparticles. Biochim Biophys Acta Proteins Proteom 1865:28–42.
666 https://doi.org/10.1016/j.bbapap.2016.10.005
667 Zeyaeyan A, Malakote M (2000) Effects of zinc application on growth and yield of wheat in calcareous soils. Soil
668 Plant 2:99–110
669 Zhang Z, He X, Zhang H, Ma Y, Zhang P, Ding Y, Zhao Y (2011) Uptake and distribution of ceria nanoparticles
670 in cucumber plants. Metallomics 3:816–822. https://doi.org/10.1039/c1mt00049e